Wavelet Analysis of Transient Biomedical Signals and Its Application to Detection of Epileptiform Activity in the EEG

Hansjerg Goelz, Richard D. Jones and Philip J. Bones

Key Words
EEG Spike Detection
Matching Pursuit Methods
Wavelet Analysis

INTRODUCTION

Wavelet-based signal analysis has evolved as a highly innovative strategy in applications where it is desirable to look at signals simultaneously in the time and frequency domains. Distinct types of wavelet transforms offer new perspectives for a wide range of signal processing applications, including compression, de-noising, time-frequency analysis and feature detection. Wavelet transforms are suited to the representation of nonstationary physiological signals such as the EEG. Similar representations cannot be achieved with the Fourier Transform or short-time Fourier Transform because they are based on analyzing intervals of a fixed length. There are different approaches to wavelet analysis: we discuss the Discrete Wavelet Transform (DWT), Continuous Wavelet Transform (CWT), and Matching Pursuit (MP) methods. It is also necessary to find the analyzing wavelet best suited for one's application. Interpretation of the transformed data is more complicated than for the Fourier Transform.

In the first part of this paper we present a general and illustrated introduction to wavelet analysis. Special attention is given to the way transient waveforms are represented under the various transforms and potential pitfalls are highlighted with EEG-related examples. In the second part, we illustrate the application of some of these techniques to one of our areas of particular interest - automated detection of epileptiform activity in the multichannel EEG. We describe the wavelet-based stages of a spike detection system we have developed. The performance of this section of the system has been determined in a preliminary clinical study.

DISCRETE WAVELET TRANSFORM

An orthogonal expansion breaks a function down into a number of *uncorrelated* components. In a multiresolution expansion those components vary in length. The most basic orthogonal multiresolution expansion was described by the mathematician Alfred Haar as early as 1910. He found that a function $f(t)$ could be expanded into an infinite series of approximation coefficients c_k and detail coefficients $d_{j,k}$ according to

$$f(t) = \sum_{k=-\infty}^{\infty} c_k \, \phi(t-k) + \sum_{k=-\infty}^{\infty} \sum_{j=0}^{\infty} d_{j,k} \, w(2^j t - k)$$

where $\phi(t)$ and $w(t)$ are nowadays known as the scaling function and the corresponding wavelet function respectively (Figure 1).

This expansion can be regarded as a transform to a new basis formed by shifted (or *translated*) and scaled (or *dilated*) instances of $\phi(t)$ and $w(t)$. For digital signal processing we can derive a very short and efficient filter pair from these functions: $\phi(t)$ corresponds to a low-pass filter (LP) and $w(t)$ to a high-pass filter (HP).

Both filters are applied to a signal and subsequently downsample the resulting signals by a factor of two, by removing every other sample. We have effectively split up the signal into an approximation signal and a detail signal (Figure 2). Note that the overall number of samples is retained. When the previous step is repeated for the approximation signal several times, we end up with a single approximation signal and a series of detail signals. This procedure is called a *discrete wavelet transform* (DWT) or *multiresolution decomposition.*

The first approximation signal is similar to a signal sampled at half the original sampling rate. The second approximation corresponds to a quarter of the original sampling rate, and so on. High frequency details in the approximation signal are gradually lost as we progress through the levels of the decomposition. In fact, these details are carefully retained in the detail signals, so the original signal can be reconstructed from the wavelet coeffients. The inverse transform is performed in a series of steps consisting of upsampling (inserting zeros between samples), LP filtering and addition of the detail signals. This is another attractive feature of the DWT beside its computational speed.

When the frequency characteristics of the Haar wavelet filters are studied (Figure 3, top left), we find that the low-pass and the high-pass overlap considerably. How can the sepa-

H. Goelz, DipPhys, is a Ph.D. candidate, Department of Electrical and Electronic Engineering, University of Canterbury, Christchurch, New Zealand; R.D. Jones, M.E., Ph.D., FACPSEM, FIPENZ, SMIEEE, is a Biomedical Engineer and Neuroscientist, Department of Medical Physics and Bioengineering, Christchurch Hospital, Christchurch, New Zealand; P.J. Bones, M.E., Ph.D., MACPSEM, SMIEEE, is an Associate Professor, Department of Electrical and Electronic Engineering, University of Canterbury, Christchurch, New Zealand.

Requests for reprints should be addressed to Dr. Richard D. Jones, Department of Medical Physics and Bioengineering, Christchurch Hospital, Private Bag 4710, Christchurch, New Zealand

Presented at the Inaugural meeting of the EEG and Clinical Neuroscience Society (ECNS) at the George Washington School of Medicine, October 21-23, 1999, Washington, D.C.

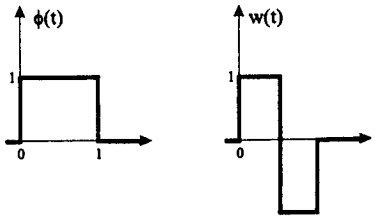

Figure 1.
Scaling function $\phi(t)$ and corresponding wavelet function $w(t)$ of the Haar wavelet.

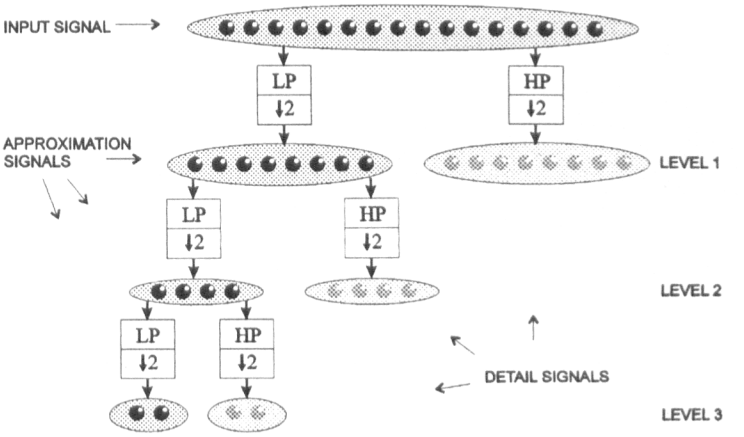

Figure 2.
Multiresolution Decomposition structure. The input signal is filtered with a pair of filters (LP and HP) and subsequently downsampled. The result is an approximation and a detail signal. The procedure is repeated several times for the approximation signal.

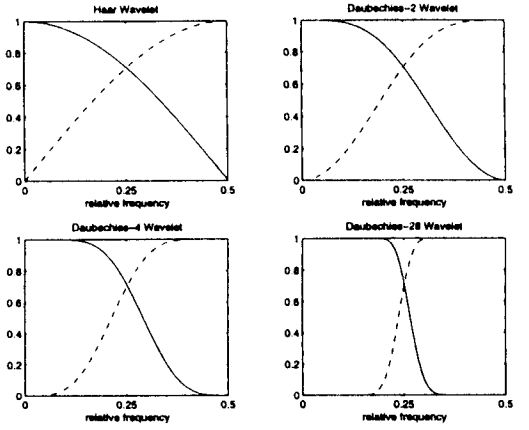

Figure 3.
Frequency characteristics of the Haar wavelet filter pair and the Daubechies' wavelets filter pairs of order n = 2, 4 and 28 (solid lines: low-pass, dashed lines: high-pass). The quality of the band separation increases with the order of the wavelet.

ration of the two bands be improved? It is extremely difficult to find a filter pair that meets all the boundary conditions required for the DWT. In the late 1980s Daubechies' discovered a family of wavelets that combine optimal band-separation (or maximal "flatness" of the filter characteristics) with short filter lengths. These wavelets are commonly referred to as Daubechies-*n* wavelets, where *n* indicates the order of the wavelet. The Haar wavelet is equivalent to the Daubechies-1 wavelet. The filter characteristics of the Daubechies' wavelets of order 2, 4, and 28 are also shown in Figure 3.

Each coefficient in a DWT corresponds to a certain waveform in the original signal. We have reconstructed the waveform of a single detail coefficient from level 5 (Figure 4). These waveforms represent the actual wavelet functions of the Daubechies' wavelet family. No analytic expression exists for the wavelet functions, but they can be approximated recursively to any accuracy. Figure 4 shows how the number of oscillations increases with the order of the wavelets. However, a large number of oscillations in a filter also has drawbacks. It may add oscillations to transient events in the signal in applications like de-noising, a technique in signal processing that reduces the noise level without modifying the information in a signal. There is a trade-off between the amount of band separation we can achieve and the number of oscillations in the corresponding filter pair.

Figure 5 shows the frequency characteristics of a complete 4-level decomposition with the Daubechies' wavelet. The high-pass of the level-1 details is the same as in Figure 3. The detail signal of levels 2, 3, and 4 have a band-pass characteristic. This is the result of a low-pass filter, a downsampling step and a high pass filter in the downsampled domain. Some sidelobes may be seen in the low-pass and band-pass for order n = 2 (Figure 5, top). These sidelobes correspond to a crisp waveform (top left in Figure 4). Although the sidelobes do not appear in the frequency characteristics in the filter pair (Figure 3) they are added by the downsampling step in the DWT. In a higher order of the wavelet (e.g., n = 28) the sidelobes disappear and a cleanly cut partitioning of the entire spectrum is obtained (Figure 5, bottom).

The main advantages of the DWT are high computational speed and invertability. A range of wavelets for the DWT have

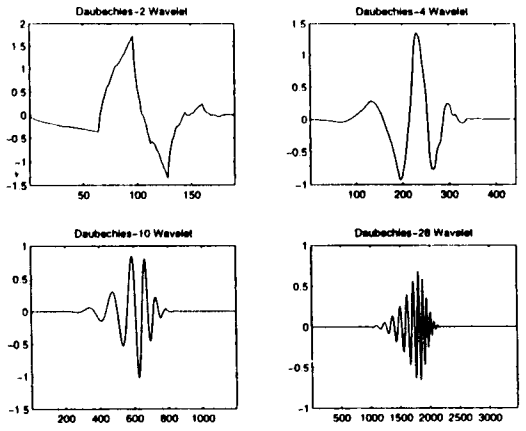

Figure 4.
Level-5 reconstructions of Daubechies' wavelets filters of order n= 2, 4, 10, and 28.

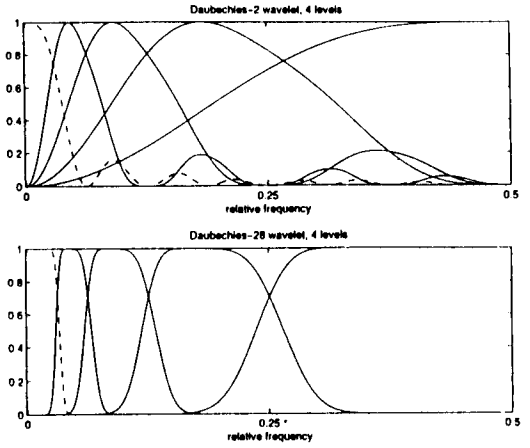

Figure 5.
Band-pass characteristics of 4-level wavelet decomposition (dashed lines: approximations, solid lines: details) for Daubechies' wavelets filters of order n= 2 (top) and n=28 (bottom).

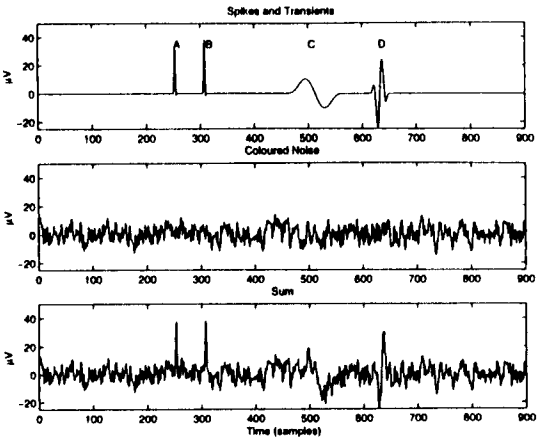

Figure 6
Four transients "A" to "D" (top row), pink noise (middle row) and test signal (bottom row) composed of the sum of both. The simulated waveforms represent two monophasic spikes, one biphasic spike and a slow artifact. The test signal is equivalent to 4.5 s of EEG sampled at 200 Hz.

been found since Daubechies' discovery. They include near symmetric and symmetric waveforms. Major applications of the DWT are data compression and de-noising.

TRANSIENT DETECTION

To illustrate the means by which wavelet analysis can be used to help in the detection of epileptiform spikes, a test signal with transient and background features has been devised. This will be looked at via the short-time Fourier Transform and two types of wavelet transforms, with a particular emphasis on the properties of the transforms with respect to transient detection.

First, four transient waveforms are added to "colored" noise (Figure 6). Transients *A* and *B* are derived from the same waveform but feature slightly different amplitudes. The colored noise is derived from low-pass filtered white noise. Note the variety of small transients in the colored noise.

The Short-Time Fourier Transform (STFT) of the test signal is examined first. The STFT is, for example, what is used in a *compressed spectral array.*[2] We used a window width of 64 samples (320 ms) and split the test signal into 27 windows (50% overlap). Transient *D* is clearly visible in the STFT (Figure 7), while the other transients generate weak responses only. Transients *A* and *B* are spread out over a wide range of frequencies. Transient *C* is too wide to fit into any of the windows and is thus spread over several temporal windows.

When the window width is reduced to 32 samples (55 windows) we get stronger responses for the short transients *A* and *B* (Figure 8). Now even the fourth transient does not fit into a single window. Thus, all four transients cannot be detected with a single window size appropriately.

Next the DWT (Daubechies-2 wavelet, see Figure 4) is applied to the signal (Figure 9). All transients are more clearly visible in the detail signals of the DWT than in the previous STFTs. Specifically, transients *A* and *B* correspond to the only outstanding peaks in the level 1 detail signal. Since smaller scales correspond to shorter windows and larger scales to wider windows all transients can be detected through a single transform. Transient *C* is represented by the approximation signal. Significantly, transients *A* and *B* are represented differently in detail signals 2 and 3 although they were generated from the same waveform. This is one of the major drawbacks of the DWT for our application: it is not translation-invariant. A transient in the signal causes a specific pattern in the transform but this pattern will change as soon as we shift the signal by a couple of samples. Thus,

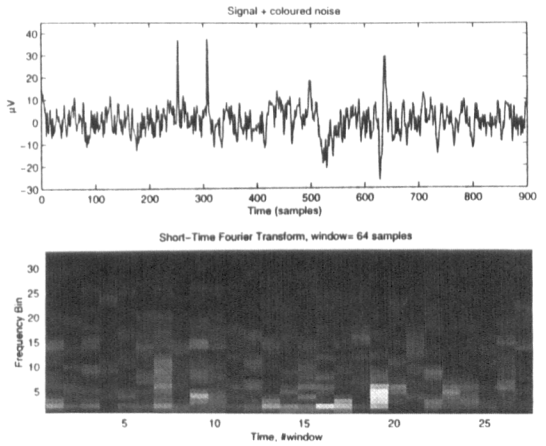

Figure 7
Test signal (top row) and modulus of the Short-Time Fourier Transform with window width 64 samples.

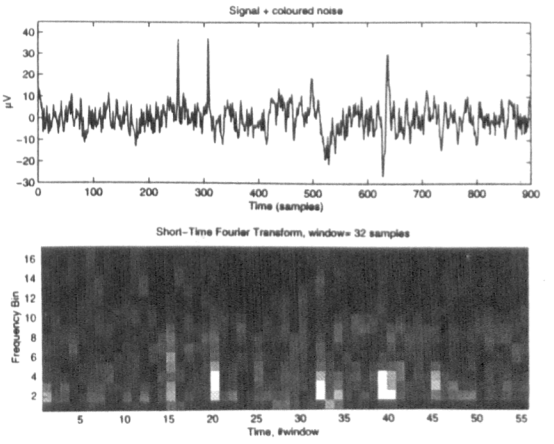

Figure 8
Test signal (top row) and Short-Time Fourier Transform with window width 32 samples.

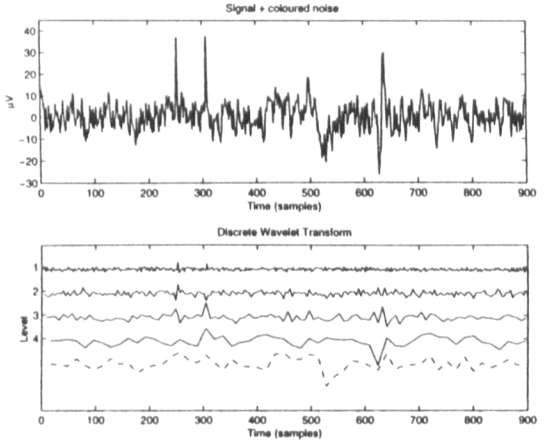

Figure 9.
Test signal (top row) and 4-level Discrete Wavelet Transform with Daubechies-2 wavelet (frequency bands in this Figure correspond to those in Figure 5). Note that transient two is not detected by the same scale as transient one, despite the two being identical in form.

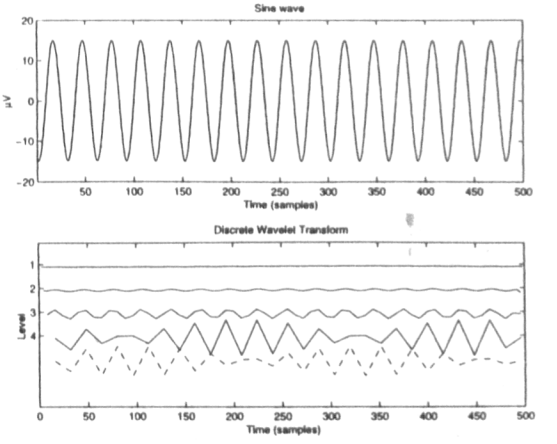

Figure 10.
Sine wave (top row) and Discrete Wavelet Transform with Daubechies-2 wavelet (frequency bands in this Figure correspond to Figure 5). A strong interference between the wavelet and the sine wave becomes evident. Although the frequency of the wave is well localized, we cannot rely on a detection in a specific scale at any time instance.

although a transient may be detected, a tansient-specific feature cannot be extracted from the DWT.

Illustration of the lack of translation-invariance is even clearer in Figure 10 in which the DWT of a sine wave is shown. The cycles of the sine wave are represented by the level-4 details and the approximation intermittently, forming what is in effect an interference pattern. Note the high amplitude of the wavelet coefficients when they are in phase with the wave. At any one time we could not rely on a detection pattern for a cycle or half-cycle of the wave.

CONTINUOUS WAVELET TRANSFORM

Unfortunately, it is not possible to design a transform which is translation-invariant, orthogonal and invertible at the same time. Of these attributes, translation-invariance is the most important for spike detection. We therefore chose to use the continuous wavelet transform (CWT) in our design. The CWT of a signal can be considered as the output of a series of band-pass filters. A modulated window function is chosen as a prototype filter called the *analyzing wavelet*. To cover the whole spectrum the analyzing wavelet is re-scaled to a series of scales. No samples are dropped as in the DWT. With the CWT one can explore scales and frequencies in individual steps, whereas the DWT can only provide one scale per octave, corresponding to each level. Wavelet filters for the CWT can be generated by sampling the analyzing wavelet at various rates.

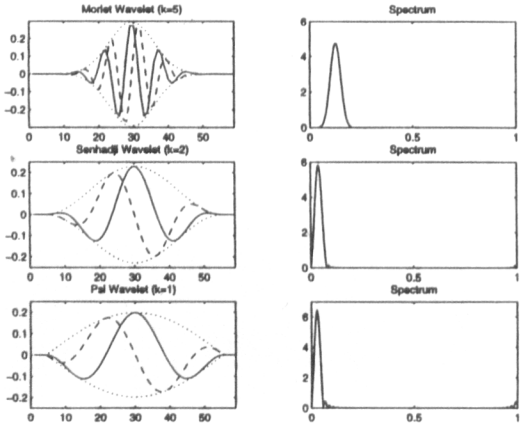

Figure 11.
Complex-valued wavelets: Morlet-wavelet (top row), Senhadji's wavelet (middle row) and psi-1 wavelet (bottom row). Waveforms on left side (solid line: real part, dashed line: imaginary part, dotted lines: complex envelope) and corresponding frequency characteristics on right side. Note that there are no mirror frequencies in the spectra because the wavelets are complex in the time domain.

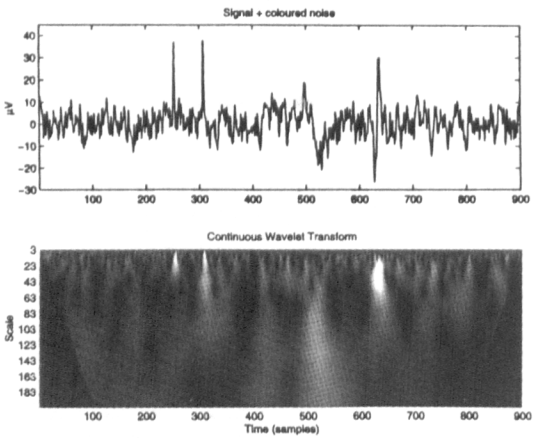

Figure 13.
Continuous wavelet transform of the test signal.

The result is a redundant representation of the signal. We end up with a larger number of wavelet coefficients than the signal samples fed into the transform. However, by doing this the chances of finding our target pattern are increased. A window function is modulated by multiplying with sine and cosine waves, which shifts the spectrum of the window function. Three complex wavelets are illustrated in Figure 11. Choosing the complex-valued Morlet wavelet[3] (Figure 11, top row) allows achievement of an optimal time-frequency resolution. For spike detection application a wavelet featuring a smaller number of oscillations is required. A modulated Hanning window as proposed by Senhadji et al.[4] (Figure 11, middle row) for epileptiform spike detection this is a good

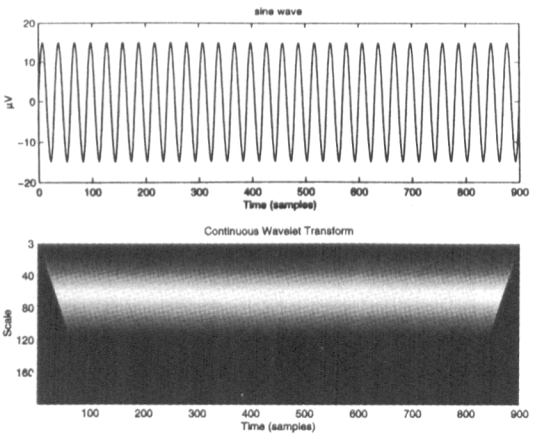

Figure 12.
Modulus of the Continuous Wavelet Transform of a sine wave using Senhadji's wavelet. Note that the transform is virtually independent of time.

choice. The smallest possible number of oscillations is achieved with the psi-1 wavelet (Figure 11, bottom row).[5]

The output of a CWT is also referred to as a *scalogram* since its vertical axis relates to scale rather than frequency. Scales are inversely proportional to frequencies with a proportionality factor, which is dependent on the wavelet filter. For a complex-valued wavelet filter the modulus (or absolute value) of the resulting complex wavelet coefficients is commonly depicted in the scalogram. Figure 12 shows a scalogram for a sine wave, with barely noticeable interference between the analyzing wavelet (Senhadji's wavelet) and the wave. The scalogram is fairly constant over time because the complex wavelet can accommodate all phases of the oscillation. A discrete set of scales is used, rising linearly from a scale of 3 to 201. The strongest response can be seen at scale 70.

All four transients can clearly be seen in the scalogram of the test signal (Figure 13). The response to transients *A* and *B* is now very similar. Transient *C* corresponds to the maximum wavelet coefficient at scale 100. Even transient features of the background can be traced in the dendrite structure of the scalogram. The CWT gives a more detailed, redundant, translation-invariant representation of the data. Unfortunately, its computational complexity is orders of magnitude larger than that of the DWT and there is no simple method to invert the CWT like the DWT. One compromise is to oversample the DWT to achieve relative invariance to translation. For a review of such variants with application to analyzing seizure EEGs see Schiff et al.[6] Only the CWT allows for the application of a complex modulated window function as an analyzing wavelet, which results in a continuous estimate of signal power in a frequency band without phase interference.

MULTISCALE FEATURES OF TRANSIENTS

The foregoing section has provided a basis for detection of transient waveforms. In addition, it is also often desirable to

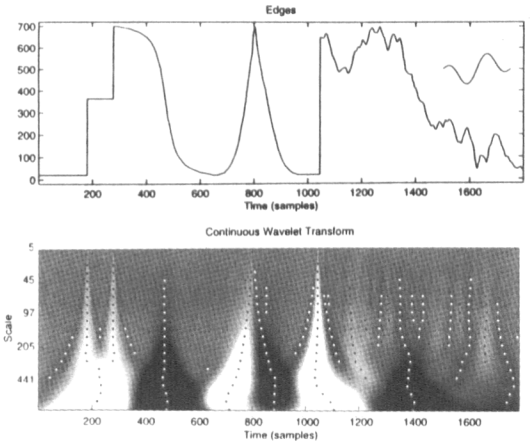

Figure 14.
Scalogram of several sharp transients (true amplitude scaling, 18 scales per octave). Local temporal maxima and minima are marked with black and white dots, respectively. The analyzing wavelet (imaginary part of psi-1) is shown in top right corner.

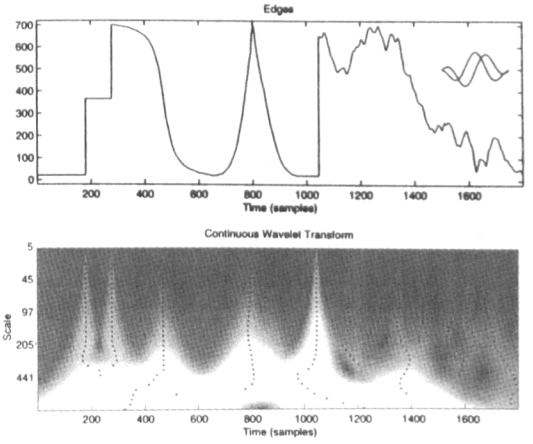

Figure 15.
Scalogram of several sharp transients as for Figure 14 but analyzed with a complex wavelet (shown in top right corner). Temporal modulus maxima were marked with black dots in the scalogram.

discriminate between and classify different transients. This can be done by extracting features of each detected transient from the scalogram. Transients of interest consist of two or more edges. Edges are well localized in time but poorly localized in frequency. Thus they may not be fully represented by a single point in the scalogram as in our previous test signal. A good strategy is therefore to trace temporal maxima in the scalogram across scales. These traces have been labeled *fingerprints* or *multiscale edges*.[7,8]

Figure 14 shows a test signal comprising a series of edges and also shows the imaginary part of the psi-1 wavelet as the analyzing wavelet. Harmonic progression of scales with 18 scales per octave was used. As the analyzing wavelet is real, both local maxima (black dots) and local minima (white dots) are marked in the scalogram. For the purpose of description each signal feature is referred to as a "transient" and each line of dots as a "multiscale edge." For each transient either (a) a single multiscale edge (samples 480, 750, 850) or (b) three multiscale edges (near samples 180, 240 and 1050) are found in the scalogram.

In Figure 15 the full complex wavelet (psi-1) has been applied. Modulus maxima are marked in the scalogram. Now only one multiscale edge is found for each transient except for the peak near sample 800. Here two edges of a sharp peak are covered by a single multiscale edge. The CWT estimates the local energy content of a signal. Only with a complex wavelet can this estimate be made independent from the phase of the signal. The phase of wavelet coefficients along the multiscale edges can be collected as additional information. Unfortunately, if noise is present in the signal (samples 1100 to 1800) it becomes difficult to trace multiscale edges. Some multiscale edges are discontinuous as we move to larger scales. For further analysis and parameter extraction from multiscale edges see Berkner and Wells.[9]

MATCHING PURSUIT

In the Fourier Transform, frequencies are covered by changing the modulation of the prototype function. In the CWT the scale of the prototype function is changed instead. For the CWT a wavelet with a fixed modulation is chosen which will be sufficient for many applications. The variety of features in the EEG is, however, large and includes oscillatory elements just like transients. Let us for example take a look at some alpha spindles.

Figure 16 shows a bipolar recording from the occipital region that contains several alpha spindles. In the scalogram the spindles are clearly visible but their frequency cannot be determined very well. It could be somewhere between 7.5 and 12.5 Hz. An isolated transient near sample 850 is also found in the scalogram.

In Figure 17 the modulation of the analyzing wavelet has been changed from $k = 2$ to $k = 8$. Now one can obtain the alpha frequency with reasonable precision as being close to 9 Hz. At the same time the transient event near sample 850 disappears from the scalogram. So is it possible to combine both analyzing wavelets in a single analysis? In 1993 Mallat and Zhang[10] proposed a new method called *matching pursuit*, which is not limited to a single analyzing wavelet. It has, instead, a dictionary of waveforms, all of which are normalized to unit energy. The signal is filtered with all waveforms and the sample with the largest magnitude among all responses is chosen. An instance of the corresponding waveform is translated and scaled appropriately and is called a *time-frequency atom* of the signal. The atom is subtracted from the signal and added to a reconstruction signal. The

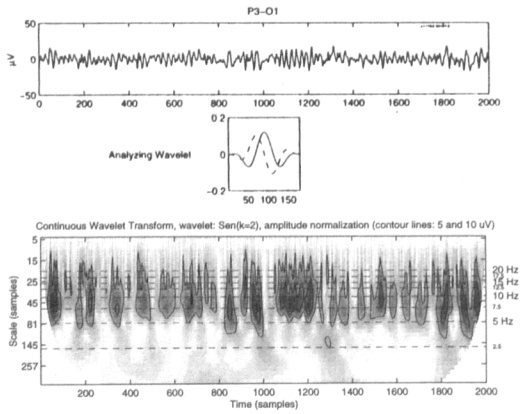

Figure 16.
Series of alpha spindles in bipolar EEG recording (10 s, 200 Hz sampling rate) and corresponding scalogram. Senhadji's wavelet, modulation k=2, 6 scales per octave. A frequency scale is added on the right hand side of the scalogram. Sharp edges of the alpha spindles reach into higher frequencies.

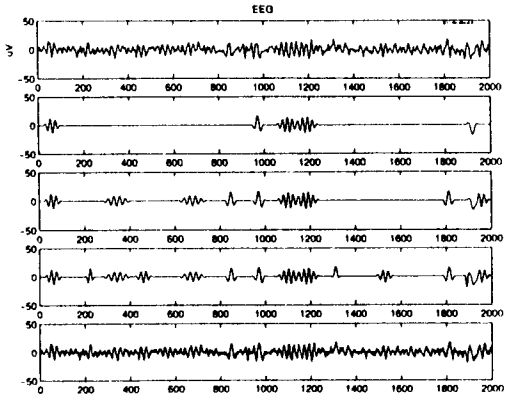

Figure 18.
An example of matching pursuit. The dictionary included 20 scales with 4 modulations each of Senhadji's wavelet. Original signal (top row) followed by reconstruction signal after 5, 10, 15, and 20 iterations. Original signal is superimposed on 20-th iteration reconstruction in bottom row.

procedure is repeated until the difference between original and reconstruction becomes sufficiently small.

In Figure 18 the EEG trace was analyzed with a dictionary of 71 waveforms. They included 20 scales (4 per octave) and 4 modulations (k=1,2,4,6) of Senhadji's wavelet.[4] The reconstruction signal is plotted after 5, 10, 15, and 20 iterations. After 5 iterations an alpha spindle is found near sample 1150 in the reconstruction. It is represented by two adjacent time-frequency atoms. Therefore, the most central peak of the spindle is attenuated in the reconstruction. The spindle would be better represented by a larger modulation (e.g., k= 8 or 10). The isolated transient near sample 850 appears in

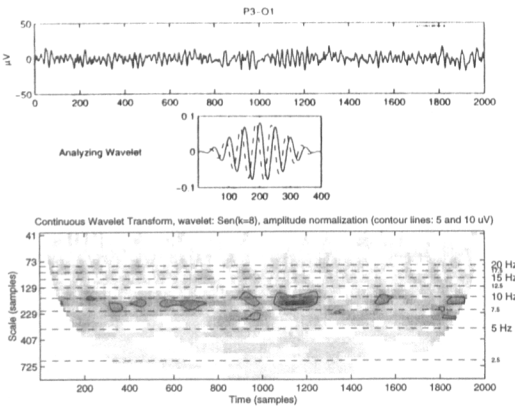

Figure 17.
Series of alpha spindels in bipolar EEG recording and corresponding scalogram.

the reconstruction after 10 iterations but its characteristic sharp edges are lost. The sharp edge details would eventually be picked up by atoms in further iterations. As one could see in the previous section, edge details are distributed across scales. With matching pursuit, a sharp edge would be decomposed into several atoms.

Matching pursuit is the best way to see both "the forest *and* the trees" in a signal but it is a computationally very expensive algorithm. In this example, the signal had to be filtered 1420 times to extract 20 time-frequency atoms and, hence, is an order of magnitude slower than the CWT. For the application of matching pursuit to sleep spindles see Durka and Blinowska[11] and Zygierewicz et al.[12]

DETECTION OF EPILEPTIFORM ACTIVITY

Since the early 1970s many approaches have been taken to find a reliable detection method for epileptiform discharges. However, the huge variety of age and status related EEG patterns and artifacts[2,13] makes it extremely difficult to build such a system. Most spike detection systems use some form of feature extraction stage followed by a classification stage. Gotman et al.[14,15] measured features such as sharpness and duration of individual waves and half-waves (rising and falling edges) in attempting to mimic the EEG reader's approach. Glover et al.[16] and Dingle et al.[17,18] combined the mimetic feature extraction stage with a rule-based expert system for classification. Artificial neural networks were used by Webber et al.[19] and Gabor and Seyal.[20] James et al.[21] constructed a hybrid system incorporating on mimetic feature extraction and artificial neural networks and fuzzy logic for classification.

Soon after fast algorithms for the DWT and CWT became available,[1,6,22] their spike detection properties were explored. Kalayci and Oezdamar[23] extracted spike features from the DWT (Daubechies' wavelet, orders n = 2 and n = 20) followed by an artificial neural network for classification. Senhadji et al.[4] applied the CWT (Senhadji's wavelet, modulation

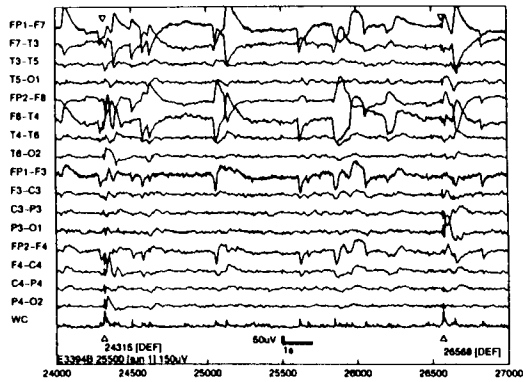

Figure 19.
Generalized interictal discharges in a 12-year old patient and average wavelet filter response over 4 scales (psi-1 wavelet with central frequencies 60, 43, 33, and 27 Hz) and over all 16 channels. Epileptiform spikes near samples 24315 and 26568 generate a stronger filter response than sharp transients caused by several eye-movements. WC: wavelet coefficients, average.

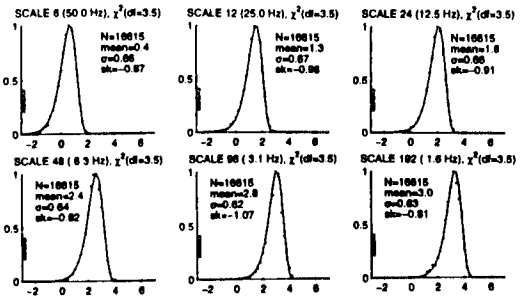

Figure 21.
Consistency of chi-square distribution of log magnitude wavelet coefficients across scales.

$k = 2$) and modeled the wavelet coefficients of background EEG with the chi-square distribution. They derived a detection threshold from the background distribution. Clarencon et al.[24] implemented the CWT (Morlet-wavelet, modulation $k = 5$, 4 scales per octave) with downsampling to reduce computational complexity. They achieved real-time operation. D'Attelis et al.[25] used a polynomial spline wavelet for the DWT. They report better detection properties for the polynomial spline wavelet than for the Daubechies-2 wavelet and an approximation of the Morlet-wavelet.

A NEW APPROACH TO DETECTION OF EPILEPTIFORM ACTIVITY

The approach we have taken to detection of epileptiform activity is based around the CWT with the complex-valued psi-1 wavelet (see Figure 11).[26] We present a statistical model for the wavelet coefficients of background EEG. Detection thresholds are derived from this background model and candidate spike features are extracted as fingerprints (multi-scale edges) from the scalogram. Events are then classified as epileptiform or artifactual.

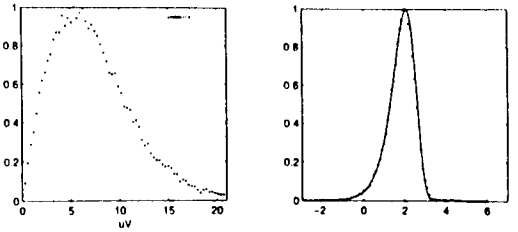

Figure 20.
Amplitude distribution of wavelet coefficients resulting from a single channel of background EEG and the Psi-1 wavelet. Distribution of modulus (left) and log modulus (right) with fitted Chi-Square distribution (df=3.5).

Before describing in greater depth the approach we have taken, it is insightful to see an illustration of the sensitivity of the psi-1 wavelet to epileptiform spikes. In the example shown in Figure 19, a 15s epoch of bipolar EEG was filtered with the psi-1 wavelet at four scales. The magnitude of the resulting wavelet coefficients was averaged across the four scales and 16 channels. The average of the wavelet coefficients ("WC") show strong peaks for two interictal discharges but only small variations for eye-blinks and eye-movements.

Distribution of Wavelet Coefficients for Background Activity

The distribution of wavelet coefficients of a 214s epoch of background activity from an occipital bipolar channel is shown in Figure 20 (left); there were no artifacts or alpha spindles on this channel. A chi-square distribution is fitted to the amplitude distribution and *degrees of freedom (df)* estimated from the mean and variance of the wavelet coefficients, providing values of $df = 2.4$ to $df = 6.4$. Taking the log magnitude of wavelet coefficients leads to a distribution that is less skewed (Figure 20, right); *df* can then be adjusted to match mean, standard deviation and skewness to the log distribution. The best match is found for $df = 3.5$. The resultant distribution of wavelet coefficients of background activity is remarkably consistent across scales (Figure 21).

This consistency has also been shown to hold across channels and individuals. Thus, the log wavelet coefficient of a sharp transient can be related to the mean of the log background distribution and, hence, estimate the probability that a given wavelet coefficient occurs by chance. We could call this the "Richter scale for transients in the EEG."

Transient Detection

Epileptiform transients are detected as a deviation from the background distribution in a range of scales. Local maxima with a log amplitude of 1.4 or more above the mean background are marked in the scalogram for an epileptiform transient in Figure 22 and called *single scale transients* (SSTs). An SST indicates an unusual event in the signal and also defines a time-frequency atom.

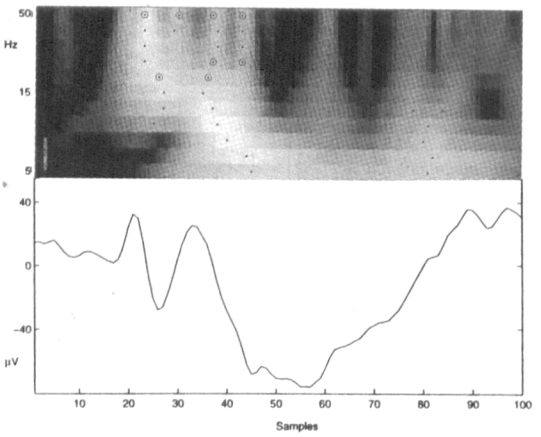

Figure 22.
Close up of an epileptiform transient (spike and wave complex) and corresponding scalogram (11 scales, 3 scales per octave). Local maxima that significantly exceed the background distribution are marked with dots in the scalogram. Dots are marked by circles are referred to below (Figure 23).

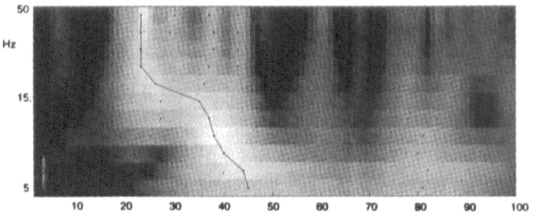

Figure 24.
The most important SSTs for each transient are traced across scales. The resulting structure is called "time-scale fingerprint" (FP).

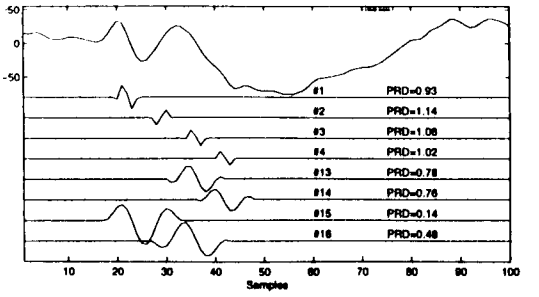

Figure 23
Spike wave complex and waveforms of eight SSTs (those marked by circles in Figure 22). The Percentage Root-Mean-Square Difference (PRD) is shown for each single scale transient (SST). SSTs #1 to #4 reflect high slope aspects of transients in the signal. SST #15 features a small PRD and, hence, represents a substantial part of the spike.

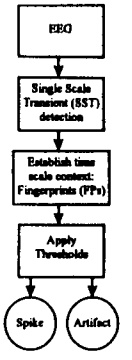

Figure 25.
Stages of the spike detection system: EEG recordings are analyzed by the SST detector. FPs are formed from detected SSTs. Linear discriminant analysis is used to improve the selectivity of the system.

Figure 23 shows eight selected SSTs from Figure 22 and the waveforms of the corresponding time-frequency atoms. The Percentage Root-mean-square Difference (PRD) of the atoms' waveforms with respect to the original waveform is calculated. The PRD helps identify SSTs that *closely represent* parts of the signal. In Figure 23 SST #15 has a small PRD since it closely fits the waveform of the spike. SSTs #1 to #4 indicate a high amount of activity in the 50 Hz band. However, the high PRD of these SSTs indicates that the generating activity is not centered at 50 Hz. In contrast, muscle spikes show up as SSTs with small PRDs in the 50 Hz band.

Feature Extraction

In Figure 24 the most important SSTs have been linked across scales. This structure is called *time-scale fingerprint* (FP).[7] For each SST in the fingerprint amplitude, phase, translation, scale, log amplitude (with respect to mean background) and PRD are recorded. The root mean square of the log amplitudes is calculated for each FP.

Thresholds are applied to the root mean square of the log wavelet coefficients and PRDs. The peak amplitude of the FPs are evaluated in the following way: if the peak occurs at the smallest scale (highest frequency) it is rejected as a potential muscle artifact. Conversely, if the peak is found at the largest scale (lowest frequency) it is rejected as a potential eye-blink. A spike is considered to have been detected when simultaneous FPs are seen in at least two channels (Figure 25). We have developed a fast algorithm for the CWT with the psi-1 wavelet which allows us to calculate the CWT on 11 scales and perform SST and fingerprint extraction for 16 channels three times faster than real-time on a 90-MHz PC.

Preliminary Clinical Evaluation

A preliminary evaluation of our method was carried out on 11 clinical EEG recordings with an overall duration of 278 min. The patients' ages ranged from 2 weeks to 84 years. Sixteen bipolar channels were recorded with several montages and sampled at 200 Hz. Three independent raters identified 298 definite epileptiform discharges in the recordings. Epileptiform activity was classified as generalized in 7 cases and multifocal in 4 cases. The psi-1 wavelet was used in a CWT with 11 even integer scales (3 per octave). SSTs were detected in individual scales and joined to fingerprints in each channel.

Thresholds were applied to the fingerprints. This results in a sensitivity of 84% and a selectivity of 12%.

DISCUSSION

Spike Detection

The CWT provides a reasonable statistical reference for background EEG with epileptiform transients showing up as deviations from the background on multiple scales (SSTs). Evidence from several scales can be gathered and linked in the time-scale plane (FPs). The sensitivity can be adjusted by changing the detection threshold. However, selectivity falls sharply when the threshold is lowered.

It is important to note that this preliminary investigation has performed analyses on individual channels only. Work is underway to improve the selectivity of the system by making greater use of spatial context of epileptiform activity in the EEG. Further improvements are also likely through the incorporation of wide-sense temporal context in the detection process. A larger data set will be used to separate training and test sets for the evaluation.

Wavelet Analysis

Wavelet analysis provides a powerful new means of visualizing and analyzing signals that are changing dramatically in both the time domain (raw signal) and frequency domain (spectrum). Mimetic features such as amplitude, slope and duration of EEG waves are closely related to the properties of multiscale edges found in the CWT. Wavelet analysis has been shown to mimic the early stages of human perception.[27,28] It has considerable potential as a means to improve the accuracy of the detection and identification of characteristic transients in the EEG.

SUMMARY

Wavelet based signal analysis provides a powerful new means for the analysis of nonstationary signals such as the human EEG. The properties of the discrete wavelet transform are reviewed in illustrated application examples. The continuous wavelet transform is shown to provide better detection and representation of isolated transients. An approach to extract features of edges and transients from the continuous wavelet transform is outlined. Matching pursuit is presented as a more general transform method that covers both transients and oscillation spindles. A statistical model for the continuous wavelet transform of background EEG is found. A spike detection system based on this background model is presented. The performance of this detection system has been assessed in a preliminary clinical study of 11 EEG recordings containing epileptiform activity and shown to have a sensitivity of 84% and a selectivity of 12%. The spatial context of epileptiform activity will be incorporated to improve system performance.

ACKNOWLEDGMENTS

The work of Hansjerg Goelz is supported by a doctoral scholarship provided by the University of Canterbury, Christchurch, New Zealand.

REFERENCES

1. Daubechies I. Orthonormal bases of compactly supported wavelets. Comm Pure Appl Math 1988; 41: 909-996.
2. Duffy FH, Iyer VG, Surwillo WW. Clinical Electroencephalography and Topographic Brain Mapping. New York: Springer Verlag; 1989.
3. Grossmann A, Kronland-Martinet R, Morlet J. Reading and understanding continuous wavelet transforms. In: Combes JM, Grossmann A, Tchamitchian P, (eds). Wavelets, Time-frequency Methods and Phase Space. New York: Springer; 1989; 2-20.
4. Senhadji L, Dillenseger JL, Wendling F, Rocha C, Kinie A. Wavelet analysis of EEG for three-dimensional mapping of epileptic events. Ann Biomed Eng 1995; 23: 543-552.
5. Goelz H, Roesler F, Roeder B, Hennighausen E. Segregation of spatiotemporal components of auditory event related potentials. In: Witte H, Zwiener U, Schack B, Doering A (eds). Quantitative and Topological EEG and MEG Analysis. Jena: Druckhaus Mayer Verlag; 1997; 3:238-241.
6. Schiff SJ, Aldroubi A, Unser M, Sato S. Fast wavelet transform of EEG. Electroencephalogr Clin Neurophysiol 1994; 91:442-445.
7. Witkin, AP. Scale-space filtering. Proc 8th Int Conf Artificial Intelligence 1983; 2:1019-1022.
8. Mallat S, Zhong S. Characterization of signals from multiscale edges. IEEE Trans Pattern Anal Mach Intell 1992; 14:710-732.
9. Berkner K, Wells RO. A new hierarchical scheme for approximating the continuous wavelet transform with applications to edge detection. IEEE Sig Proc Letters 1999; 6:193-195.
10. Mallat S, Zhang Z. Matching pursuits with time-frequency dictionaries. IEEE Trans Sig Proc 1993; 41:3397-3415.
11. Durka PJ, Blinowska, KJ. Analysis of EEG transients by means of matching pursuit. Ann Biomed Eng 1995; 23:608-611.
12. Zygierewicz J, Blinowska KJ, Durka PJ, Szelenberger W, Niemcewicz S, Androsiuk W. High resolution study of sleep spindles. Clin Neurophysiol 1999; 110:2136-2147.
13. Hughes JR. EEG in Clinical Practice. Boston, Mass: Butterworth; 1982.
14. Gotman J, Gloor P. Automatic recognition of interictal epileptic activity in the human scalp EEG. Electroencephalogr Clin Neurophysiol 1976; 41: 513-529.
15. Gotman J, Wang LY. State dependent spike detection: validation. Electroencephalogr Clin Neurophysiol 1992; 83: 12-18.
16. Glover JR, Raghavan N, Ktonas PY, Frost JD. Context-based automated detection of epileptogenic sharp transients in the

EEG: elimination of false positives. IEEE Trans Biomed Eng 1989; 36: 519-527.

17. Dingle AA, Jones RD, Carroll GJ, Fright WR. A multistage system to detect epileptiform activity in the EEG. IEEE Trans Biomed Eng 1993, 40: 1260-1268.
18. Jones RD, Dingle AA, Carroll GJ, et al. A system for detecting epileptiform discharges in the EEG: real-time operation and clinical trial. Proc 18th Ann Int Conf IEEE Eng Med Biol Soc, Amsterdam; 1996.
19. Webber WRS, Litt B, Wilson K, Lesser RP. Practical detection of epileptiform discharges EDs in the EEG using an artificial neural network: a comparison of raw and parameterized EEG data. Electroencephalogr Clin Neurophysiol 1994; 91: 194-204.
20. Gabor AJ, Seyal M. Automated interictal EEG spike detection using artificial neural networks. Electroencephalogr Clin Neurophysiol 1992; 83: 271-280.
21. James, CJ, Jones RD, Bones PJ Carroll, GJ. Detection of epileptiform discharges in the EEG by a hybrid system comprising mimetic, self-organized artificial neural network, and fuzzy logic stages. Clin Neurophysiol 1999; 110: 2049-2063.
22. Unser M. Fast Gabor-like windowed Fourier and continuous wavelet transform. IEEE Sig Proc Lett 1994; 1:76-79.
23. Kalayci, T, Oezdamar, O. Wavelet preprocessing for automated neural network detection of EEG spikes. IEEE Eng Med Bio Mag 1995; 14:160-166.
24. Clarencon D, Renaudin M, Gourmelon P, et al. Real-time spike detection in EEG signals using the wavelet transform and a dedicated digital signal processor card. J Neurosci Meth 1996; 70:5-14.
25. D'Attelis CE, Isaacson SI, Sirne RO. Detection of epileptic events in electroencephalograms using wavelet analysis. Ann Biomed Eng 1997; 25:286-293.
26. Goelz H, Jones RD, Bones PJ. Continuous wavelet transform for the detection and classification of epileptiform activity in the EEG. Proc 21st Ann Int Conf of IEEE Eng Med Biol Soc, Atlanta, USA; 1999.
27. Mallat S. Multifrequency channel decompositions of images and wavelet models. IEEE Trans Acoust Speech Signal Process 1989; 37:2091-2110.
28. Unser M, Aldroubi A. A review of wavelets in biomedical applications. Proc IEEE 1996; 84:626-638.